Instability and Pattern Formation in Ferrofluids

Supervised by Dr Lorenzo De Michele ld389@cam.ac.uk
Demonstrated by Ryan Brady rab228@cam.ac.uk

Part II Physics E2b Lab Report, Lent 2017

Abstract

Drops of ferrofluid injected into a surrounding surfactant solution and held in cells made of parallel glass plates were observed in a changing magnetic field. Firstly, the threshold field at which the circular drop became unstable (elliptical) was found for varying ratios of drop radius to plate separation. A dimensionless reduced variable, the Bond number, was compared to theoretical values and found to agree with the theory to within an order of magnitude. Secondly, a different ferrofluid was explored in larger quantities and at higher fields, where labyrinth patterns were formed. The ratio of labyrinth arm spacing to plate separation was used to predict a theoretical Bond number, which was again compared to the experimental value. It was also found to agree to within an order of magnitude. Finally, the effect of hysteresis for fields around the point of elliptical instability was explored for both the ferrofluids, which allowed a qualitative comparison of the different ferrofluids and their mechanical and magnetic hysteretic behaviour.

1 Introduction

A ferrofluid is a colloidal suspension of tiny ferromagnetic particles in a fluid medium, typically oil or water. The single domain nanoparticles, around 10nm in diameter, are coated in polymer to keep the particles apart and hence weaken the dipole-dipole interaction forces, which fall off as r^{-3}.[1] The particles are usually Fe_2O_3 and have a very high magnetic susceptibility.

Ferrofluids were first patented in the 1960s by Solomon Stephen Papell, and were used by NASA to manipulate rocket fuel in zero gravity.[2] Today ferrofluids are used primarily in creating airtight seals in rotating mechanical equipment.[3] They have also been used to bring drugs to a target site in the body.[4] They are often studied due to interesting

structure-formation properties, which are described by non-linear equations and depend heavily on boundary conditions. Another use for dispersions of ferromagnetic particles is in megnetorheological fluids: larger particles with stronger dipole interactions mean that the viscosity of the fluid can be significantly increased with an applied field.[5] Although not strictly ferrofluids, they are worth mentioning given the results here, where some of the ferrofluid appeared to become sticky at higher fields.

The aim of this experiment was to test the theoretical predictions of elliptical instability by Tsebers[6] and Langer[7], to test the theory of labyrinth spacing by Rosenweig [8], and to explore hysteresis with respect to a double energy minimum as explored by Hillier and Jackson.[9] These theoretical predictions are outlined in Section 2. Section 3 gives a summary of the experimental methods used, while Section 4 details the results. Section 5 includes the discussion of results, errors and potential improvements that could be made. The overall conclusions of the experiments are presented in Section 6.

2 Theoretical Background

2.1 Relevant Magnetostatic Concepts and The Bond Number

Ferromagnetic materials contain magnetic dipoles which align themselves with an applied external field, leading to an enhancement of the field. The magnetisation M of a magnetic material is a measure of its net dipole alignment. Therefore for an external field of strength H_0, the field within the material can be written $H = H_0 - MD$ where D is a demagnetising coefficient which is shape-dependent.[10]

Although ferromagnetic materials in general are non-linear at relatively low field strengths,[11] here we assume that the ferrofluid behaves linearly as $M = \chi_H H$, where χ_H is the magnetic susceptibility. This allows us to write the magnetic energy U_m as:

$$U_m = -\frac{\mu_0}{2}\int_V \frac{\chi_H H_0^2}{1+\chi_H D} dV \tag{1}$$

It can be shown that the linear approximation for a non-linear fluid keeps equation (1) valid to first order with respect to M/H.[6] The surface energy will be $U_s \simeq \gamma t \mathrm{d}x$ where γ is the interfacial energy, t is the plate separation and $\mathrm{d}x$ is the surface (perimeter) of the drop (for circular drop $\mathrm{d}x \propto r^2$).[12]

The two competing factors in the analysis of the ferrofluid's stability are the magnetic and surface energies. The Bond number N_b [7] is a dimensionless quantity which is a measure of the balance of the two energies U_m and U_s:

$$N_b = \frac{\mu_0 H_0^2 t}{2\gamma} = \frac{B_0^2 t}{2\mu_0 \gamma} \tag{2}$$

2.2 Elliptical Instability (Langer and Tsebers)

When a field is applied to a circular drop, Tsabers[6] assumes that the first unstable shape it will take is an ellipse. As this happens, the surface area dx of the drop will increase, leading to an increase in U_s. The demagnetisation coefficient D will increase, causing U_m to decrease. Therefore we consider a threshold Langer Bond number N_b^L for when U_m is large enough compared to U_s to cause a shape distortion. This is plotted in Figure 1.

$$N_b^L = 9(1-k^2)k\left[k^3 + (1-k^2)(8-3k^2)K(k^2) + (7k^2-8)E(k^2)\right]^{-1} \tag{3}$$

Where:

$$K(m) = \int_0^{\pi/2} \left(1 - m\sin^2(\theta)\right)^{-1/2} d\theta \tag{4}$$

$$E(m) = \int_0^{\pi/2} \left(1 - m\sin^2(\theta)\right)^{1/2} d\theta \tag{5}$$

And where k is a parameter which characterises the height of the drop (which is equal to plate separation t) compared to it's radius r:

$$k = \frac{(2r/t)}{\sqrt{1+(2r/t)^2}} \tag{6}$$

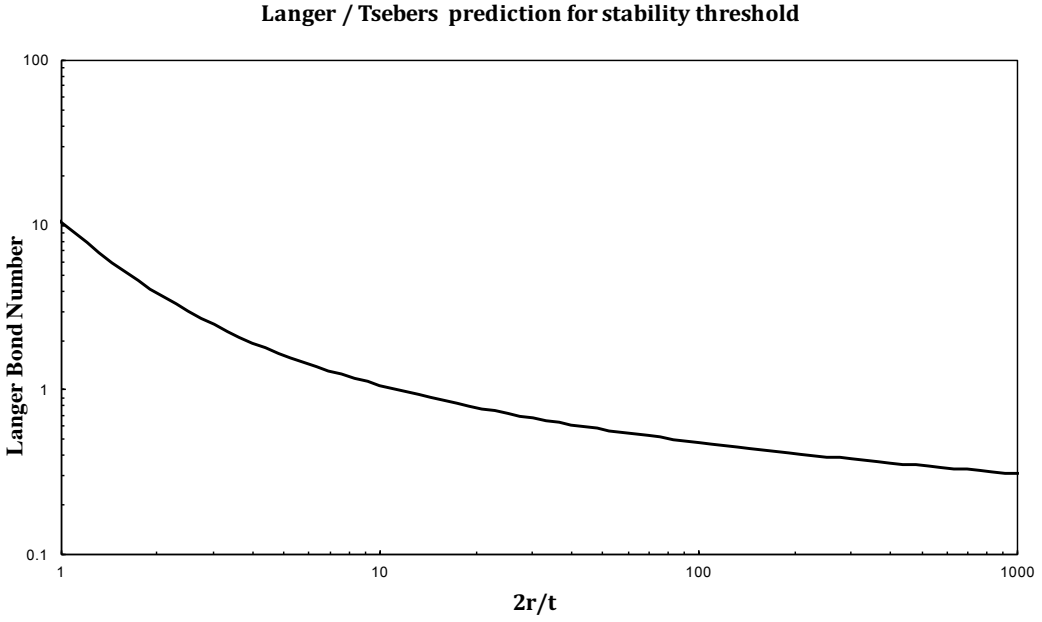

Figure 1: The theoretical threshold Langer Bond Number N_b^L from equation (3) as a function of $2r/t$ and plotted on a logarithmic scale.

2.3 Labyrinth Spacing (Rosenweig)

Once the ferrofluid drop has become unstable at higher fields, it is observed to form labyrinth patterns with 'fingers' of magnetic fluid invading the surrounding surfactant. As the field is increased the fingers split into multiple branches and eventually form the labyrinth pattern with stripes of definite thickness. Rosenweig[8] derived a semi-empirical theory of labyrinth spacing which relates the Bond number N_b^R to the stripe aspect ratio $z = (\text{stripe width})/t$. This is plotted in Figure 2.

$$N_b^R = \frac{\frac{\pi}{\chi_H^2 z^2}\left(1 + \frac{2\chi_H}{\pi}\left[\tan^{-1} z + \sum_{n=0}^{N}\left(\tan^{-1}(2za) - \tan^{-1}(2zb)\right)\right]\right)^2}{\left(\frac{1}{1+z^2} + \sum_{n=0}^{N}\left(\frac{a}{1+(2za)^2} - \frac{b}{1+(2zb)^2}\right)\right)} \tag{7}$$

Where:

$$a = (n+1)\rho + n + 3/2 \tag{8}$$

$$b = (n+1)\rho + n + 1/2 \tag{9}$$

Here N is the number of stripes over which the series sums are carried out (number of nearest neighbours) and ρ is the lane/stripe ratio.

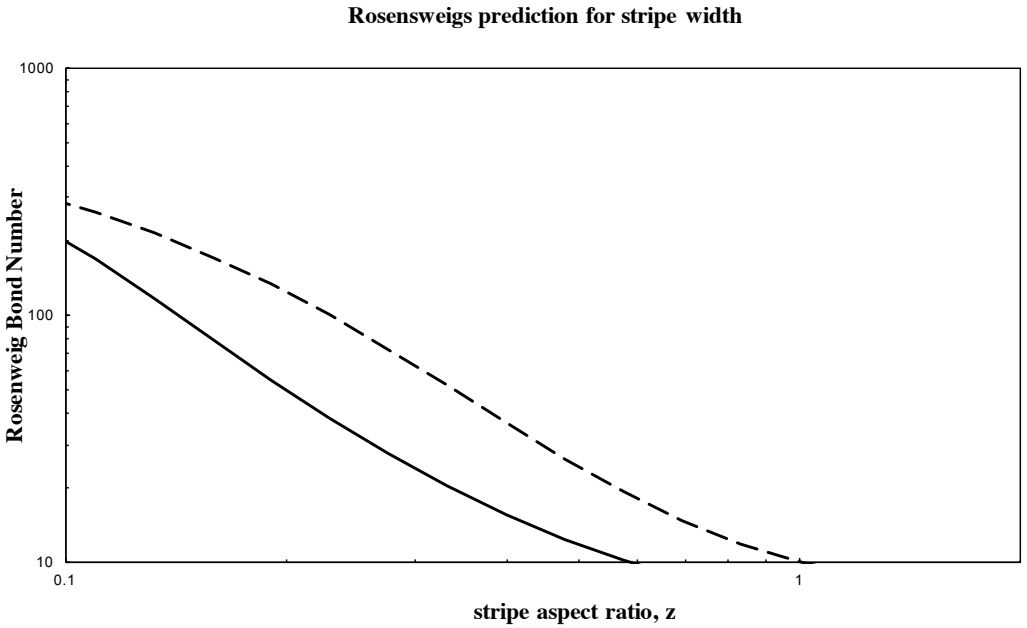

Figure 2: The theoretical Rosenweig Bond number N_b^R from equation (7) as a function of z for $\chi_H = 1.9$, $N = 3$, $\rho = 5$ (solid line) and $\chi_H = 1.9$, $N = 10$, $\rho = 1$ (dashed line). These are around the typical values obtained in this experiment.

2.4 Hysteresis

Ferromagnets in general are highly hysteretic.[11] Hillier and Jackson[9] present a theory which states there is an energy barrier which separates the circular drop from the ellipse/finger state minima, therefore forming a double minima. As a result there should be a hysteresis loop when plotting eccentricity against applied field.

3 Method

3.1 Experimental Set-up

A parallel plate cell was constructed to contain the ferrofluid drops in the surfactant solution. The two optically flat glass plates were cleaned using water, ethanol then acetone, each time wiping thoroughly using lens wipes to ensure there were minimal impurities on the glass surfaces. This was to prevent surface interactions with the ferrofluid that could introduce unwanted systematic errors. The smaller glass plate was mounted on specially designed metal cell mounts of varying heights, allowing for variation of plate separation. It was sealed using a thin smear of grease, with the plate pressed down at the edges to prevent the liquid leaking as well as to ensure the height was consistent (the layer of grease height was assumed negligible).

The Triton X-100 0.1% surfactant solution (with a known surface tension of 30.0 ± 0.2 mNm^{-1}) was evenly distributed on the lower plate using a pipette, and the ferrofluid was drawn up into a syringe then injected into the solution using a fine needle. This allowed for a good control over the size and distribution of the ferrofluid drops. Despite the drops sometimes drifting, small bar magnets were used to move them around or to remove excess ferrofluid by splitting the drops. The top plate was then gently lowered on top of the filled cell, using toothpicks to help keep the plate level with the surfactant. Occasionally air bubbles were trapped between the plates but if they were large enough to interfere with the experiment or to cause the ferrofluid to smear, then the glass was re-cleaned and the cell re-filled.

Once prepared, the cell was placed inside a horizontally mounted electromagnet. The electromagnet was a Helmholtz Coil which was water-cooled and could produce a uniform perpendicular magnetic field. The strength of the field was controlled by varying an input current. The set up was lit from below by a bulb, and a USB camera was clamped above. Images were captured and analysed using ImageJ. A diagram of the set up is shown in Figure 3.

Throughout this experiment two different ferrofluids were used, referred to in this report as "old" and "new". Although the supplier claimed that they would be identical, they exhibited considerably different tendencies to stick, with the new ferrofluid readily sticking to the glass at higher fields, often making it difficult to take good data.

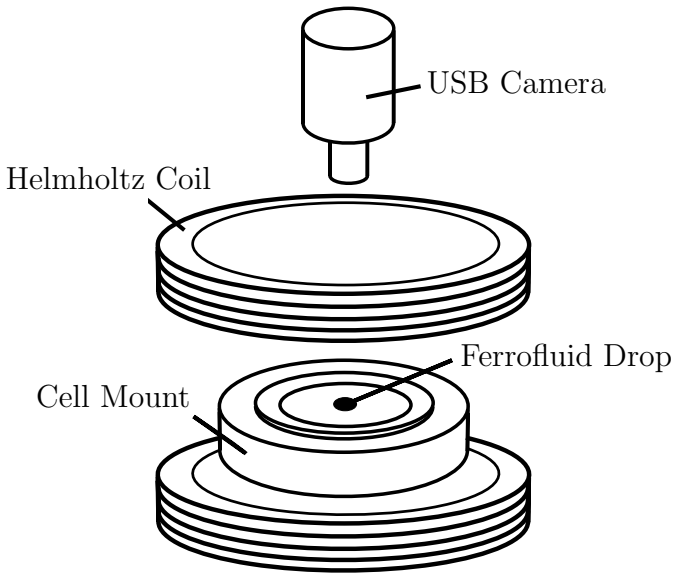

Figure 3: Diagram of the experimental set up. The coils were connected to a power supply and ammeter, and the camera to a computer running ImageJ software. There was a small bulb just below the lower coil to provide light for the images. This image is my own and was created using inkscape.

3.2 Preliminary Measurements and Calibrations

ImageJ processed images in pixel length scales, so a pixel to mm calibration was required to give a useful output from the software's inbuilt measuring tools. A glass plate with a dot marked in the centre surrounded by concentric circles with radii of 1,2,3,...mm was placed on the cell mount. An image was taken and a line drawn across the diameter of 4 rings, passing through the dot in the centre. This gave a mm/pixel conversion ratio with appropriate error due to the thickness of the rings. This calibration was repeated when switching to another set of equipment with a different electromagnet and camera mount height.

The magnetic field strength was measured using a zeroed Hall probe secured just above the centre of the cell. The current was slowly increased from zero and an ammeter was used to measure the current rather than using the imprecise scale on the power supply. Magnetic field strength is plotted against the measured current in Figure 4. It was found to be highly linear as expected, so the gradient was taken as a conversion factor which allowed for images to be taken at an applied current. This was much easier than trying to measure the field every time. Although there is a small offset from zero at the intercept, this was small compared to the error in each current reading, so was ignored. It is possible there was a field at zero current due to spontaneous ferromagnetism but this error is negligible compared to others.

Both the pixel and field calibrations had to be done twice as there was a problem with the current in the coil of the first electromagnet used to collect elliptical data. Although fine

for elliptical measurements, the setup could only achieve about half the desired current for creating labyrinths, so it was necessary to move to another electromagnet and camera setup between the two experiments.

Finally, the thickness of the lower glass plates were measured at multiple points across the surfaces using callipers, and were found to be 2.00 ± 0.05 mm (calliper resolution). The plate separation was then the quoted step separation of the cell mount minus the thickness of one glass plate.

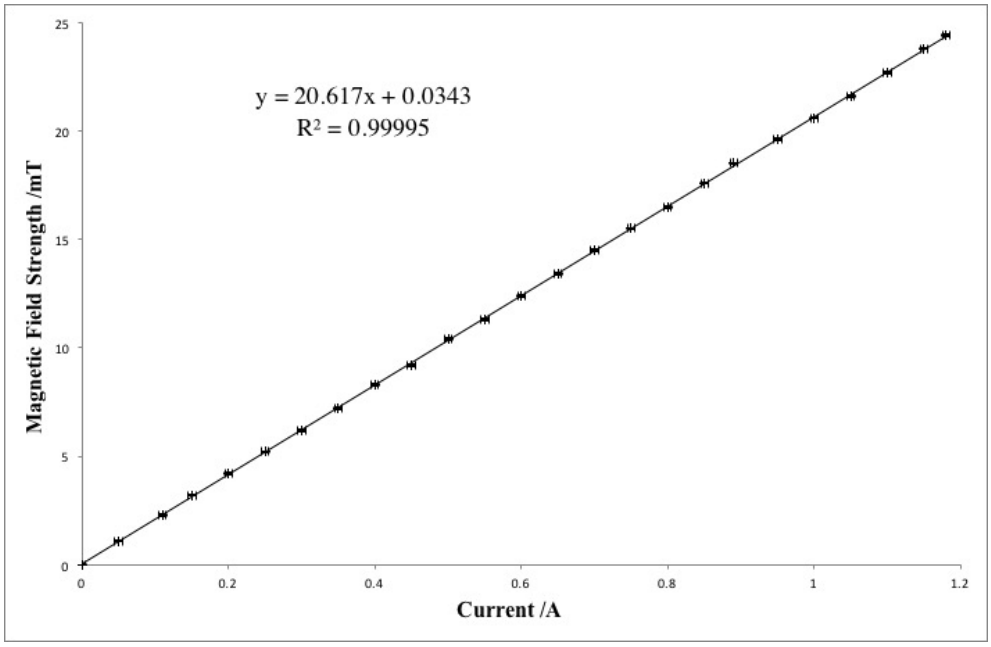

Figure 4: The calibration curve for magnetic field strength. Using excel the gradient conversion factor was found to be (20.62 ± 0.03) mTA^{-1}.

3.3 Measuring Elliptical Instability

Initially the new ferrofluid was used to create circular drops in the cells. A major problem with the new ferrofluid was it's inclination to stick to the glass, especially at higher magnetic fields, and particularly if the drop was large. If the drop didn't stick, it would often drift in the applied field. In order to overcome these issues, the drops were constantly checked using small bar magnets, allowing for the fluid around to be moved around without splitting the drop or permanently altering its shape.

Starting at zero field, images were taken of the drops as the field was increased at gradual intervals. The drop was given at least 20 seconds to settle after the field was changed, although it was sometimes favourable to leave the drop for less time to stop it from sticking, or to prevent it from drifting too far. Nearing the point of instability the drops started to bulge, and at this point the field was increased very slowly to try and ensure the error in finding the current at the point of instability was no greater than the resolution of the

Quantity	Value
Mount Heights	$[2.498 - 3.494] \pm 0.0005$ mm
Glass Thickness	2.00 ± 0.05 mm
ImageJ distance conversion	0.024 ± 0.0002 mm/pixel
Magnetic Field/Current conversion	20.62 ± 0.03 mTA^{-1}
Triton X-100 0.1% Surface Tension	30.0 ± 0.2 mNm^{-1}
Magnetic Susceptibility χ_H	1.9
Quoted Surface Tension of ferrofluid	34 mNm^{-1}

Table 1: Table of initial calibrations and known values with errors if known.

ammeter. Once the drop was clearly elliptical, the field was then reduced back in a time-symmetric manner, with images being taken in the same way. Hysteresis measurements are discussed further in Section 3.5.

Once the images were acquired, ImageJ's inbuilt measuring tools gave the major and minor axis measurements for each ellipse. This gave both drop radius r as well as a method to quantify exactly when the drop became an ellipse. Eccentricity $e = (1 - \frac{min^2}{maj^2})^{1/2}$ was the parameter used, and this was plotted against the applied current. The point of instability was often obvious from the graph, but for consistency the first point at which $e \geq 0.4$ was taken as the upper bound for determining the threshold current and hence field. As the Langer Bond number N_b^L is a function of $2r/t$, a variety of sizes of drops and plate separations were used in taking these measurements. Once again, the range of $2r/t$ values was limited mainly by the stickiness of the new ferrofluid, with large $2r/t$ ratios proving difficult to take good data with.

3.4 Examining labyrinth Arm Widths

The same general method was used to form labyrinth patterns, except higher quantities of ferrofluid were required to get a good number of stripes. Since higher fields are needed to form labyrinths, careful steps were taken to ensure the current was not switched on for too long, which prevented the coil from overheating. After quite a few attempts at forming labyrinth patterns with the new ferrofluid, it was found to be almost impossible to stop the fluid sticking to the extent that obtaining any workable data was unrealistic. The decision was made to switch to the old ferrofluid, which had virtually no problems with sticking.
The images were analysed using ImageJ, and an excel spreadsheet was made which could conveniently take the output from ImageJ and give the stripe and lane widths of the line drawn across N neighbours. These lines were drawn across neighbours as parallel as possible to ensure consistency. See Figure 9 for examples of reasonably parallel lanes.

3.5 Investigating Hysteretic Properties of the Ferrofluids

Hysteresis was investigated alongside the elliptical instability measurements, with the field being reduced incrementally back down below the point of instability. Using the new ferrofluid, the eccentricity often did not return to zero even for zero field due to the sticking effect. This large systematic error was a problem because it became impossible to determine what was magnetic hysteresis and what was mechanical sticking. For this reason, five additional hysteresis measurements were taken with the old ferrofluid, allowing for a good comparison between the two fluids.

In all cases the same surfactant solution Triton X-100 0.1% was used. A 0.01% solution with a higher surface tension was trialled, but it only worsened the sticking problem so no data taken with the 0.01% solution is present in this report.

4 Results

4.1 Summary

Quantity	Value
γ (Elliptical, new ferrofluid)	11.1 ± 1.0 mNm^{-1}
γ (Labyrinth, old ferrofluid)	18.7 ± 1.0 mNm^{-1}

Table 2: Table of results

4.2 Elliptical Instability Results

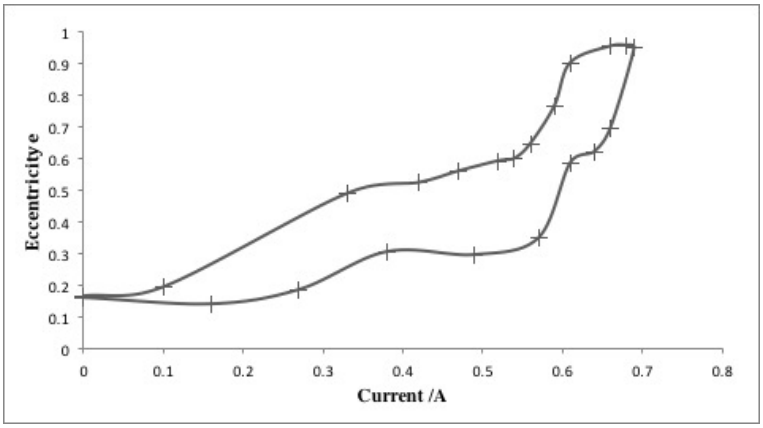

Figure 6: A typical plot of eccentricity e against current I. This also demonstrates the hysteretic effect. The lower line is for increasing field, and the top line (higher eccentricity) is for reducing the field back down.

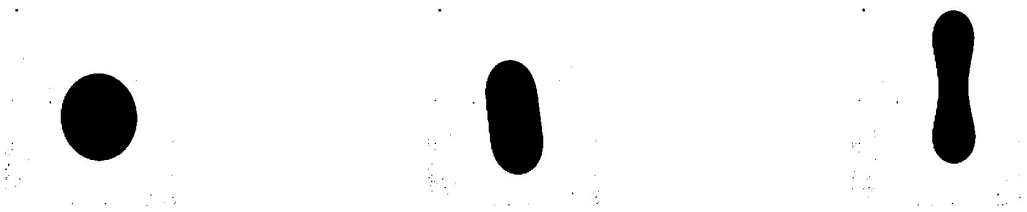

Figure 5: An example of a circular drop around the point of elliptical instability. The far left image is considered not yet at the point of instability, the middle image is roughly at the point of instability, and the right hand drop is past the point of instability.

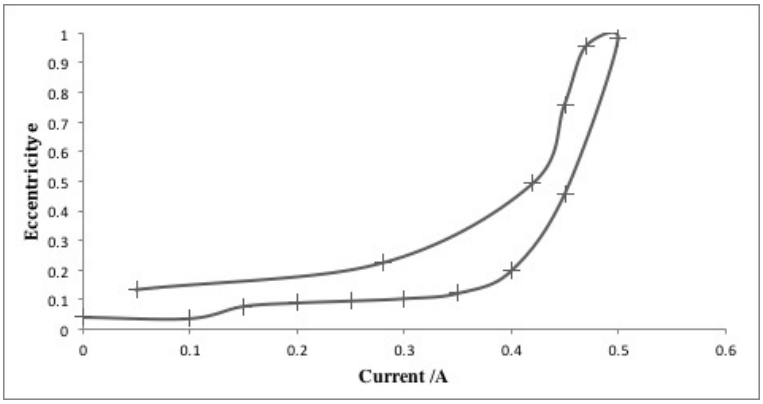

Figure 7: Another plot of eccentricity e against current I. Notice how the eccentricity does not return to zero due to a sticking effect.

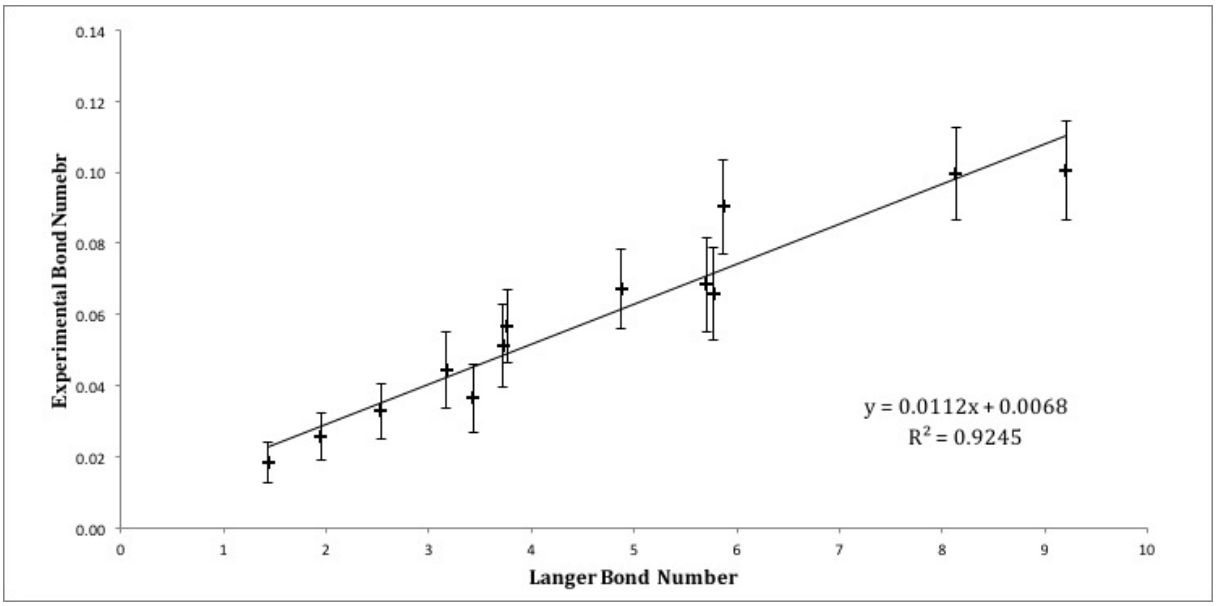

Figure 8: Plot of Experimental N_b against the Langer Bond number N_b^L for the point of elliptical instability of the new ferrofluid. Here $\gamma = 11.1 \pm 1.0$ mNm^{-1}.

4.3 Labyrinth Spacing Results

Figure 9: Examples of different labyrinth patterns formed. Left: small amount of fluid, medium field. Middle: Large amount of fluid, high field. Right: Large amount of fluid, low field.

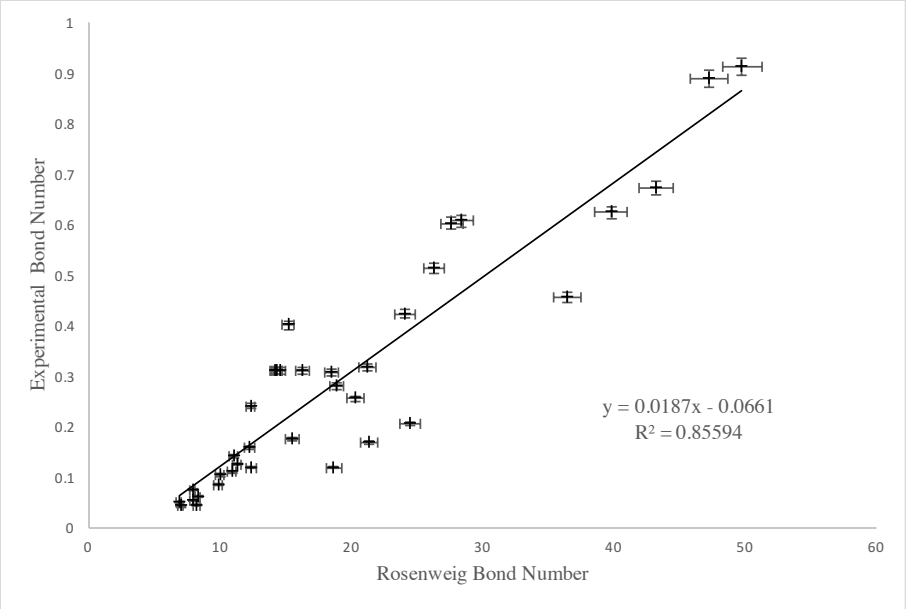

Figure 10: Plot of Experimental N_b against the Rosenweig Bond number N_b^R for different labyrinths. Here $\gamma = 18.7 \pm 1.0$ mNm^{-1}.

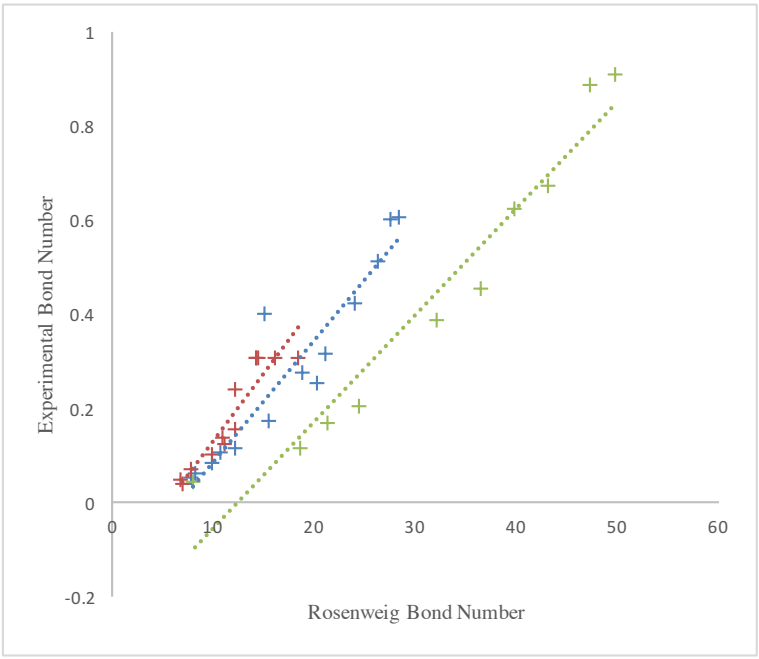

Figure 11: The same data as in Figure 10 plotted for the different plate separations. t is: 0.498mm (Red), 1.002mm (Blue) and 1.454mm (Green). R^2 values are 0.87, 0.89 and 0.94 respectively.

4.4 Hysteresis Results

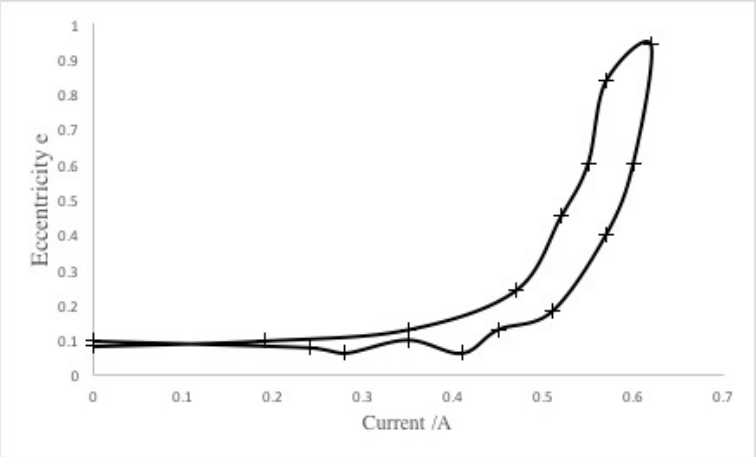

Figure 12: Plot of the magnetic hysteresis using the old ferrofluid, which resulted in a lower loop area and a return to zero eccentricity.

5 Discussion

5.1 Discussion of Results

For elliptical instability, the experimental data was found to agree qualitatively with the theory for the Langer Bond number N_b^L, shown by a reasonable straight line plotted in Figure 8, with an R^2 value of 0.92. Some points were excluded due to large systematic errors during the taking of the data, for example the fluid becoming stuck, or an air bubble interfering with the shape of the fluid. The interfacial energy γ was calculated to be $\gamma = 11.1 \pm 1.0$ mNm^{-1}. Theoretically γ can be approximated as the difference between the surface tension of the ferrofluid and the surface tension of the surfactant solution, which from Table 1 can be calculated to be around 4 mNm^{-1}. Although the obtained experimental value is roughly three times higher, it is of the same order of magnitude. Since the only qualitative relationship given in the lab book theory[10] is that they should be of the same order of magnitude, these results can be said to verify the theory. For a more qualitative relationship further theory should be explored, and a more precise knowledge of the properties of the ferrofluid and surfactant solution would be needed.

The data for the labyrinth patterns is shown in Figure 10. Once again the experiment agrees with the theory, a straight line being plotted for the experimental Bond number N_b against the Rosenweig Bond number N_b^R. The value of γ obtained was $\gamma = 18.7 \pm 1.0$ mNm^{-1}. The R^2 value is slightly lower at 0.86, and it is clear that the data is more scattered. The value of γ is around five times higher than the predicted value, but it is still within an order of magnitude so can be said to justify the theoretical prediction. It is also worth mentioning that the old ferrofluid was used, so it is likely that the two

fluids have a different value of γ, especially considering how differently they behaved. It is difficult to be more quantitative considering our limited knowledge of the fluid, and simple theoretical predictions.

One thing noticed while plotting data was that for a different plate separation t, the individual R^2 values were higher when taken separately. This is shown in Figure 11. Potential reasons for this are discussed in the next section.

Finally, the presence of hysteresis was confirmed for both the ferrofluids. For the new ferrofluid, as shown in Figures 6 and 7, a lot of this was due to sticking, as the eccentricity often did not return to zero as expected. When the old ferrofluid was tested, the eccentricity did return to around zero, and the loop areas were generally much lower. So much of the hysteresis shown by the new ferrofluid was mechanical rather than magnetic. Nevertheless, there was still always a hysteretic effect which can be assumed to be magnetic, and was confirmed by taking multiple data sets. This is in agreement with the predictions of Hillier and Jackson. A typical hysteresis loop is shown in Figure 12.

5.2 Errors

The errors bars were calculated by considering the formula for N_b (equation (2)) and by combining the errors (Table 1) in the usual way. By far the largest source of error for the elliptical data came from determining exactly where the circular drop became an ellipse, as the eccentricity changed very rapidly for a small change in field, so this error was higher than the precision of the ammeter. The Error in γ was calculated using linear regression analysis in excel.

The error bars for the labyrinth data were smaller since we were not considering a point of instability, so the error in the current was just from the ammeter precision. However it is clear that since most of the points and their errors lie outside of the best fit line, systematic errors are more likely to be the major problem with this data set. It is likely that the problem is to do with the plate separation t because the R^2 values for mounts of different heights taken separately are higher, and the data sets have quite different slopes and intercepts. This is shown in Figure 11. It is hard to know exactly why this happened and it is possible that it is nothing to to with the separation, rather the volume of ferrofluid used. If too much ferrofluid was used then a kind of inverse labyrinth was formed, which must have different boundary conditions to the assumptions in the theory. It is also possible that the plates were drawn apart slightly due to the higher fields and volumes of ferrofluid creating a larger force on the top plate, perhaps to different extents for different amounts of ferrofluid or for different values of t.

5.3 Further Comments and Potential Improvements

A general point is that fewer data points were taken throughout this experiment than desired due to the sticky ferrofluid causing more attempts at taking data to fail than be successful. The stickiness limited the range of $2r/t$ values which could be obtained, as large drops of new ferrofluid were unworkable. The effect of this was to truncate the graph in Figure 8. It was probably a mistake to switch to the old ferrofluid so late in the experiment, and if repeated then perhaps a higher surfactant concentration could be used

to prevent sticking.

The sticking effect could also have been explored quantitatively as a separate experiment, which would allow for a deeper insight into the mechanical hysteresis. Finally, the mid-range fields between the point of elliptical instability but before large labyrinth patterns were formed have been neglected in this experiment. The number of branching arms formed after elliptical instability could have been investigated at different fields. Hysteresis effects could have also been explored at higher fields.

6 Conclusion

The results of this experiment validate the theoretical predictions of Langer, Tsebers and Rosenweig. First a circular drop was examined around the point of elliptical instability and it's threshold Bond number was compared to a theoretical prediction. Using γ as a fitting parameter, the theory was found to fit the experiment to within an order of magnitude.

Next, labyrinth patterns were examined and stripe to lane ratios were used to construct another theoretical Bond number which was then compared to the experimental Bond number in the same way. This was also found to agree with the theory, and the value of γ was around the expected value. Great care was taken to reduce systematic errors throughout this experiment, but there is likely some kind of systematic error in the data taken for the labyrinth patterns, most likely relating to plate separation.

Finally a qualitative evaluation of hysteresis patterns was carried out which verified the double energy minima theory of Hillier and Jackson.

References

1. J. M. D. Coey, *Magnetism and Magnetic Materials* p545 (Cambridge University Press 2010)
2. Concept Zero, *A Brief History of Ferrofluid* (2014) https://www.czferro.com/news1/2014/10/27/history-of-ferrofluids
3. K. Raj & A. F. Chorney, *Ferrofluid Technology - An Overview* (Indian Journal of Engineering & materials Sciences 1998)
4. Y. Morimoto, M. Akimoto & Y. Yotsumoto, *Dispersion state of protein - stabilized magnetic emulsions* p3024 (Chem. Pharm. Bull. vol.30 1982)
5. A. Spaggiari, *Properties and Applications of Magnetorheological Fluids* (Dept. of Engineering Sciences and Methods, University of Modena and Reggio Emilia 2013)
6. A. O. Tsebers & M. M. Maiorov, *Magnetohydrodynamics*, 16, 21 (1980)
7. S. A. Langer, R. E. Goldstein, D.P. Jackson, *Dynamics of Labyrinthine Pattern Formation in Magnetic Fluids* (Physical Review A, 46, 8, 1992)
8. R. E. Rosenweig, *Labyrinthine Instability in Magnetic and Dielectric Fluids* (Journal of Magnetism and Magnetic Materials 39, 127, 1983)

9. N. J. Hillier & D. P. Jackson, *Width of a Ferrofluid Finger: Hysteresis and a Double Energy Minimum* (Physical Review E 75, 036314, 2007)
10. *Instability and Pattern Formation in Ferrofluids*, Part II Physics lab manual (University of Cambridge 2016/17)
11. C. Ford, *Part IB Electromagnetism*, p109 (University of Cambridge 2015/16)
12. E. Terentjev, *Part II Soft Condensed Matter*, p72, chapter 3 (University of Cambridge 2016/17)